New Journal of Physics
The open access journal at the forefront of physics

Deutsche Physikalische Gesellschaft DPG
IOP Institute of Physics

Published in partnership with: Deutsche Physikalische Gesellschaft and the Institute of Physics

PAPER

Microwave-induced direct spin-flip transitions in mesoscopic Pd/Co heterojunctions

Torsten Pietsch, Stefan Egle[1], Martin Keller, Hans Fridtjof-Pernau[2], Florian Strigl and Elke Scheer

Department of Physics, University of Konstanz, D-78464 Konstanz, Germany
[1] Present address: IMT Masken und Teilungen AG, CH-8606 Greifensee, Switzerland
[2] Present address: Fraunhofer Institute for Physical Measurement Techniques IPM, Heidenhofstrasse 8, D-79110 Freiburg, Germany

E-mail: torsten.pietsch@uni-konstanz.de

Keywords: break junction, heterostructures, quantum point contact, spin-laser, transport spectroscopy, population inversion

Supplementary material for this article is available online

OPEN ACCESS

RECEIVED
20 June 2016

REVISED
10 August 2016

ACCEPTED FOR PUBLICATION
24 August 2016

PUBLISHED
22 September 2016

Abstract

We experimentally investigate the effect of resonant microwave absorption on the magneto-conductance of tunable Co/Pd point contacts. At the interface a non-equilibrium spin accumulation is created via microwave absorption and can be probed via point contact spectroscopy. We interpret the results as a signature of direct spin-flip excitations in Zeeman-split spin-subbands within the Pd normal metal part of the junction. The inverse effect, which is associated with the emission of a microwave photon in a ferromagnet/normal metal point contact, can also be detected via its unique signature in transport spectroscopy.

1. Introduction

In recent years, a multitude of novel devices has been proposed, which rely on the dynamic interplay between spin- and charge in metallic, magnetic nanostructures. Examples include spin-torque systems and spin-transfer oscillators, as well as spin-caloritronic- and spin-hall devices [1–5]. One of the most intriguing proposals is the realisation of a novel type of spin-based laser in metallic, magnetic point contacts between a ferromagnet and a normal, non-magnetic metal [6] or two different ferromagnets [7–11]. The underlying mechanism is the creation of a non-equilibrium spin population in energy-split spin subbands via injection of hot, spin-polarised electrons into the contact region. In a normal, paramagnetic metal (N) a Zeeman splitting lifting the spin-degeneracy of spin-subbands can be generated via the application of an external magnetic field. A larger splitting, in the meV range, can be created in contacts incorporating dilute ferromagnets (f), where the spin-bands are split due to the quantum mechanical exchange interaction. It was suggested, that stimulated emission of microwave and terahertz photons takes place upon relaxation, while the non-equilibrium distribution is maintained via continuous injection of hot electrons at current densities above 10^8 A cm^{-2}, which is experimentally feasible in the point contact geometry [7, 11]. According to the theoretical predictions, this process competes with magnonic scattering processes but not with other relaxation mechanisms, such as those involving phonons, because photon-induced transitions between spin-states involve negligible momentum transfer. Consequently, a simple two-level system may be considered, where only the spin-component of the electronic energy dispersion is relevant, while the electronic temperature does not play a role as long as inelastic scattering of electrons in the contact is spin-preserving. Therefore, at least in principal, spin-flip photoemission in magnetic heterojunctions should also be observable at room temperature [12]. If realized such all-metallic spin-flip lasing devices would provide a fundamentally new type of highly tunable, miniaturised radiation source in the GHz and THz range with giant intensity compared to state of the art semiconductor quantum cascade lasers [8, 13]. However, presently the concept of spin-flip lasing in magnetic metallic junctions rests foremost on theoretical considerations [7–9, 11], albeit some experimental evidence exists. For example Korenivski and coworkers showed non-specific emission of radiation from arrays of FePt/Cu point contacts using an integrating bolometric detector [10, 14]. Similarly, Gulayev *et al* reported radiation from large contacts (>10 μm in

diameter) between a ferromagnetic rod and a second ferromagnetic film [15–17] or an antiferromagnetic FeMn layer [18, 19] observed in bolometric measurements using a Golay cell without intrinsic spectral resolution. Although they showed that the source of radiation is partially non-thermal [19–22], it is not demonstrably associated to the above named mechanism. As it stands, there is currently no unambiguous proof of optical spin-flip radiation emitted from a magnetic hetero-junction with spectral resolution in the GHz or THz range. One of the main reasons is that non-directional photoemission from individual point contacts with spectral power densities in the order of 10^{-12} W Hz^{-1} per nm^3 active volume is difficult to detect. A different approach would be considering many point contacts in parallel to increase the intensity to a measurable quantity [10, 14, 20]. However, such arrays of identical point contacts with a size of less than 10 nm, needed to achieve the required current densities of $>10^8$ A cm^{-2}, in a resonator circuit are hard to produce and the driving currents often lead to heating and destruction of the devices. Moreover, the most fundamental issue of these devices is that metals are not normally known to be transparent for radiation in the GHz and THz range but in the very special situation of a local spin-population inversion in energy-split spin-subbands.

Instead of attempting to detect photoemission from magnetic point contacts in the expected frequency range directly by optical means, Naidyuk and coworkers resort in using transport spectroscopy to probe the inverse process, i.e. by measuring the conductance of a diffusive $SmCo_5$/Cu hetero-point contact under resonant microwave excitation [12]. They showed that both absorption and emission of a microwave photon result in a distinct change of the contact resistance with opposite sign, in accordance with scattering theory.

Here we show that microwave absorption in spin-split energy levels in magnetic point contacts of Co and Pd can be detected via transport measurements and is distinguishable from phonon- or magnon scattering via their unique signatures. Point contact spectroscopy (PCS) has been established as a versatile tool to study elementary excitations and relaxation phenomena of hot electrons in a small sample volume [23]. The method is particularly useful to determine the spectral properties of phonons and magnons via inelastic electron back-scattering. However, PCS is not well suited to investigate electron–photon interactions directly, due to the negligible momentum of the photon. Still, in magnetic heterojunctions, where the transmission of electrons in magnetic point contacts is highly spin-dependent, microwave absorption and photo emission associated to a spin-flip can be detected via PCS [6]. In contrast to previous reports, we use atomic-size ballistic hetero-contacts with a tunable cross section. In this configuration highly stable point contacts with well-defined interfaces can be prepared, while the required current densities of 10^8–10^{10} A cm^{-2} are easily achieved. Due to the small volume of the active region these atomic point contacts are not expected to emit high intensity radiation as observed in previous experiments but the sensitivity to detect the creation of a local non-equilibrium spin-population in the contact core is strongly increased.

2. Spin-flip photoemission and expected transport behaviour

In a series of reports, Kadigrobov [6–9, 13, 24, 25] as well as Gulayev [11, 26] and their coworkers developed theoretical model describing the novel phenomenon of spin-flip photoemission in magnetic point contacts. The model is based on semiclassical Boltzmann transport applied to an ideal, sharp interface between two magnetic metals in a diffusive point contact geometry. Although several assumptions are made that may not hold for realistic contacts, this simple model successfully describes the conditions under which spin-flip photoemission should be observable and it predicts distinct features in the transport characteristic of the contact. In the following we outline key aspects of the theory and review the expected transport behaviour based on the calculations in [24, 25].

The basic idea behind the proposed spin-flip photoemitter is that radiant relaxation of hot, spin-polarised electrons takes place in a two-level system, i.e. energy split spin-subbands. This situation can be achieved, when spin-polarised electrons are injected at a high rate from a ferromagnet (F) into a second dilute ferromagnet (f) or non-magnetic (N) metal. The energy splitting of spin-subbands is given by the exchange splitting in f or the Zeeman splitting in N upon the application of an external magnetic field. In both cases the relevant energy scales differ by a factor of 10^3. In the case of dilute ferromagnets, such as FePt, PdNi, CuNi, the exchange energy depends on the stoichiometry of the alloy and is typically in the order of few meV. In contrast, the Zeeman energy in paramagnetic metals at moderate fields lies in the μeV range. Since the energy splitting determines the operation frequency of the spin-flip photoemitter, two different types of devices may be realized; namely F/f contacts that emit radiation in the THz range and F/N point contacts operating at GHz microwave frequencies. Here, we focus on the latter type, where the Zeeman energy in N is tunable via the external field.

The criteria to observe spin-flip photoemission are that a spin-population inversion is created in the N metal via the continuous injection of hot electrons from F into N, while the external magnetic field is applied antiparallel to the magnetisation of the F material. The population inversion is maintained as long as the injection rate is larger than the relaxation rate. This process is illustrated in the inset in figure 1. A microwave

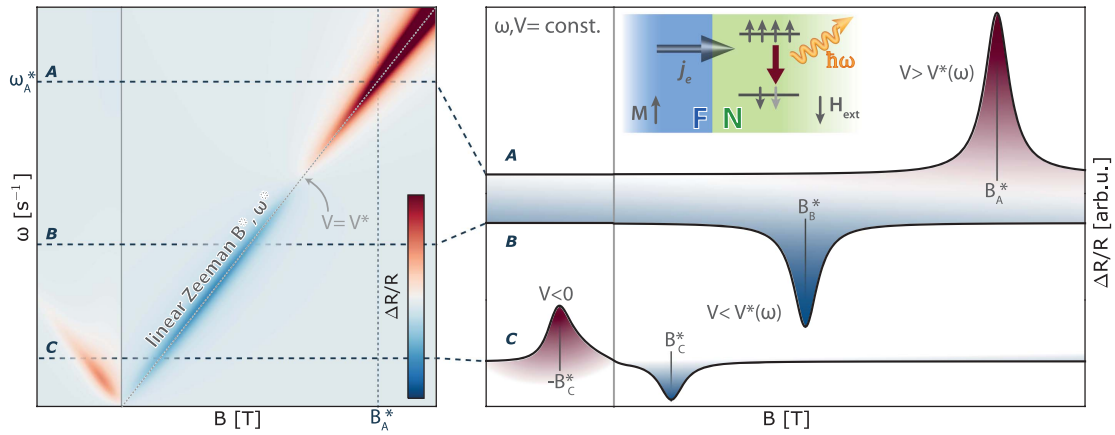

Figure 1. Expected transport behaviour of a diffusive F/N hetero-point contact due to spin-flip photoemission and absorption according to the semi-classical theory reported in [6, 12]. The left panel shows qualitatively the relative resistance change ($\Delta R/R$) as a function of applied magnetic field B and microwave frequency $\omega = 2\pi f$ at constant voltage V applied to the contact. The line traces in right panel represent sections through the resistance map at constant ω. A resistance change occurs when the resonance condition $\hbar\omega^* = g\mu_B B^*$ is fulfilled, due to the emission or absorption of a microwave photon in energy-split spin subbands (inset right panel). Although the theory considers photoemission in voltage biased point contacts, it can be expanded to account for absorption of microwave photons in unbiased contacts as well. In either case, since the energy splitting is given by the Zeeman term, a linear relationship between the resonance field B^* and frequency ω^* is expected and a distinct change of the contact resistance is predicted. A description of these resonance features at B^*, ω^* is presented in the text.

photon is emitted upon relaxation of hot electrons to the spin-ground state. In the semi-classical theory, which does not take into account details of the materials band structure, this mechanism is essentially momentum conserving and does not involve phonon mediated relaxation processes. Naidyuk *et al* [12] reported that spin-flip photoemission is not observed in the absence of microwave illumination of the contact and conclude that the process is stimulated in nature, which would give rise to a laser-like emission spectrum and justifies the use of the term *spin-flip lasing* in some of the earlier publications [7–9, 13] on the subject.

In magnetic point contacts the spin-flip of electrons upon relaxation is associated to a resistance change, even in devices with a single magnetic interface, because the backscattering probability of the electron across the interface is spin-dependent [23]. The theory developed by Kadigrobov *et al* predicts that a spin-population inversion in F/N point contacts can be identified via a distinct change in the contact resistance. Therefore electronic transport spectroscopy may be used to study the phenomenon of spin-flip lasing in magnetic, metallic junctions without directly detecting the radiation emitted from the device. The expected transport characteristics are shown in figure 1, the resistance change $\Delta R/R$ of a F/N point contact under microwave irradiation has been calculated using the formalism in references [6, 24, 25], which was recently expanded in reference [12] to incorporate the effect of a finite spin-flip rate ν_{sf} due to non-radiative spin-relaxation processes in the point of contact (PC), e.g. due to spin–orbit, phonon or impurity scattering. These processes result in a broadening of the photon resonance and a reduced amplitude of the effect. The relative resistance change due to spin-flip photoemission is then given by [12]:

$$\frac{\Delta R}{R} = \frac{4\pi\beta_{tr}^2}{3}\frac{c}{\nu_F}\frac{(\mu_B H_{rf})^2}{\epsilon_F \hbar\nu_{sf}}(n_0 V_{PC})\left(\frac{2e^2}{h}R\right)\arctan\left(\frac{2\xi}{1-\xi^2+\left(\frac{\hbar\omega - g\mu_B B}{\hbar\nu_{sf}}\right)^2}\right). \quad (1)$$

Here β_{tr} is a transport parameter, whose experimental value is approximately 0.3, c and ν_F denote the speed of light and Fermi velocity in N respectively, while ϵ_F is the Fermi energy. The amplitude of the resistance change at resonance, is also determined by the magnetic field component of the external microwave stimulus H_{rf}, the point contact volume V_{PC}, the electron density n_0 in N and the dimensionless parameter $\xi = \omega\nu_F/\nu_{sf}c$. The left panel in figure 1 shows the relative resistance change ($\Delta R/R$) as a function of applied magnetic field B and microwave frequency $\omega = 2\pi f$ at constant voltage bias V applied to the contact to inject a spin-polarised current from the ferromagnet F into the normal metal N. The line traces in the right panel in figure 1 represent sections through the resistance map at constant ω. A resistance change occurs when the Zeeman splitting matches the photon energy ($\hbar\omega^* = g\mu_B B^*$), due to the emission or absorption of a microwave photon in energy-split spin sub-bands. Since the energy splitting is given by the Zeeman term in (1), a linear relationship between the resonance field B^* and frequency ω^* is expected. In principle, the effect should be unipolar in magnetic field applied antiparallel to the magnetization in F. In the calculations shown in figure 1 we assume a fixed magnetisation direction of the F electrode independent of the external field; a positive magnetic field direction

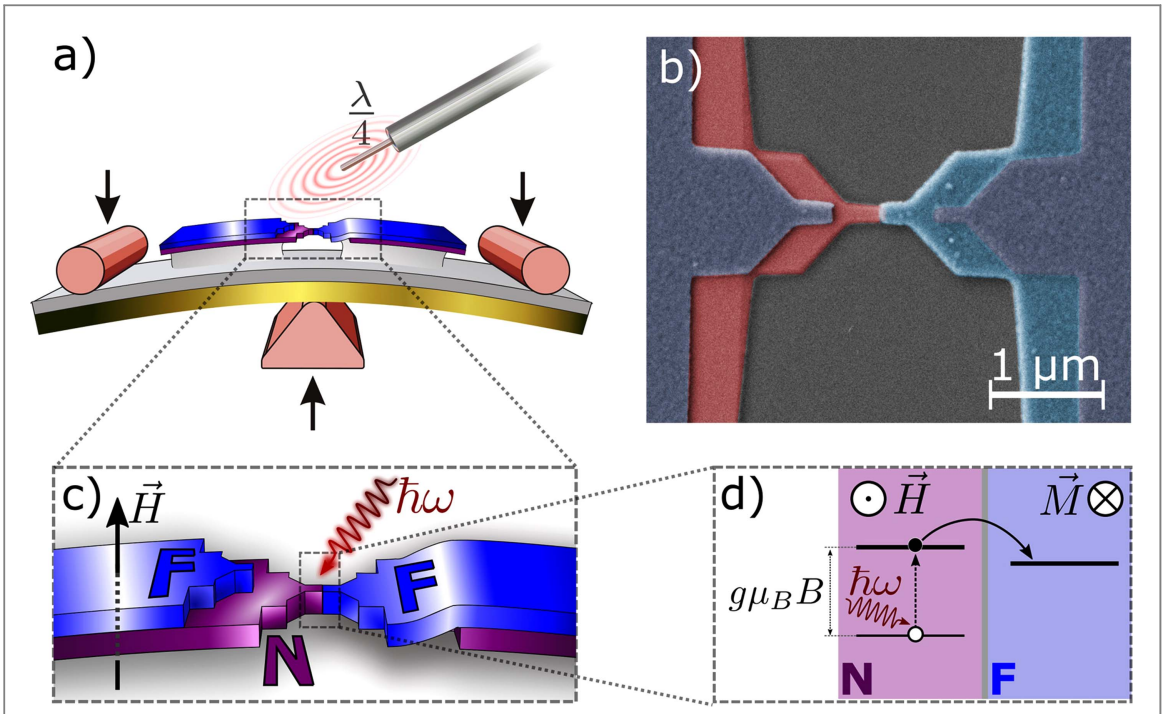

Figure 2. Tunable hetero point contacts are prepared using the mechanically controllable break-junction technique, where a suspended, microfabricated metal bridge is carefully bent to adjust the contact size. (a) Schematic illustration of the heterojunctions mounted in a three-point bending mechanism. (b) SEM micrograph of a Pd/Co heterocontact prepared via shadow evaporation of Co and Pd before opening the junction. The image has been coloured for better distinction of the different materials. (c) The contacts are irradiated by a microwave field via a $\lambda/4$ antenna in the vicinity of the sample. The magnetoconductance of the Co/Pd interface is probed via electronic transport spectroscopy at a fixed microwave frequency and -power. (d) Spin-flip transitions via absorption of microwave photons in Zeeman-split density of states in the normal metal results in a photocurrent over the N/F interface, which are detected via transport spectroscopy.

denotes the antiparallel configuration, while a negative field is directed parallel to the magnetisation in F. At strong forward bias, above a certain threshold voltage $V > V^*$, a spin-population inversion due to the injection of a spin-polarised current into N, leads to the stimulated emission of a microwave photon associated to an increase of the PC resistance (trace A in figure 1). Absorption of a microwave photon below the threshold voltage creates a photocurrent across the interface, which results in a resistance change with opposite sign (trace B). The threshold voltage V^* is frequency dependent and is mainly determined by details of the contact and the constituent materials, predominantly the density of states of the spin-up and -down bands in the F and N metals respectively [6, 24, 25].

According to the theory [12] spin-flip emission and -absorption can also be observed in parallel field, as shown in trace C, when the current direction is reversed, i.e. electrons are injected from N into F. In this case the lower Zeeman level is depopulated by the current, which in turn leads to an overpopulation of the upper Zeeman level and hence a population inversion that decays via photo-emission and results in a change of the PC resistance. The width of the resonance as well as the amplitude and sign of the resistance change associated to photon emission or absorption again depend on experimental details and contact parameters [6, 25]. It is clear from the parameter ξ in (1), that the width of the resonance at fixed ω is determined by the electron's Fermi velocity and the spin-flip rate in N.

Finally a population inversion in N may be created via microwave absorption at high incident rf power in an unbiased F/N contact. In this case, a photocurrent over the F/N interface can be detected as a change in the apparent contact resistance, whose sign depends on the relative orientation of the magnetisation in F and the applied magnetic field as well as the current direction, if a finite bias is applied to the contact [12]. Here, this situation is investigated by detecting the distinct change in near-ballistic Pd/Co point contacts shown in figure 2.

3. Methods

In order to prepare clean point contacts with sufficient stability as well as reducing thermal noise on the measurement setup, all experimental trials are performed in cryogenic vacuum at low temperatures (<4 K). Tunable point contacts are fabricated via the mechanically controllable break-junction (MCBJ) technique (see figure 2(a)). In this method, metallic electrodes are patterned on a flexible substrate via electron beam

lithography and shadow evaporation of two different metals (Co and Pd); details on the preparation process are described in the supporting information (SI-1). By carefully bending the substrate in a three-point bending mechanism, the electrodes are pulled apart and the contact diameter can be adjusted with atomic precision from bulk-like to atomic dimensions and even a well-defined tunnelling gap. A major advantage of this technique is that a clean interface is produced by breaking the junction in cryogenic vacuum for the first time. Moreover, repetitive breaking and closing of the junction always exposes a new interface, which allows statistical analysis of atomic-size point contacts and provides means to adjust their structural and magnetic configuration. Figure 2(b) shows a scanning electron micrograph of a lithographically defined point contact before narrowing the contact diameter, i.e. before breaking the junction for the first time. The geometry of the sample is chosen such that we probe mainly one interface between the normal- (N) and ferromagnetic (F) materials, while the parasitic interfaces are separated from the active one by distance of more than 200 nm, which is much larger than the relevant spin-flip scattering length for Pd (7.8 nm at room temperature and 25 nm at 4 K) [27–30]. Conductance spectra of Co/Pd point contacts were recorded in a conventional dilution refrigerator (Oxford Instruments, Kelvinox MX400) at a temperature below 150 mK. The setup is equipped with a microwave guide coupled to a $\lambda/4$ antenna with a resonance frequency of 7 GHz, which is used to irradiate point contacts with a microwave field; details on the experimental setup and the transmission spectrum of the microwave guide are shown in the supporting information (SI-2). A magnetic field up to 8 T can be applied perpendicular to the sample plane (see figure 2(c)). In this geometry, we probe the conductance of the F/N interface as a function of magnetic field, microwave power, injection current and contact size. Microwave absorption in energy-split spin sub-bands in hetero point-contacts has been theoretically described recently [6]; the proposed mechanism is sketched in figure 2(d). In a point contact between a normal metal (N) and a ferromagnet (F), an external magnetic field is applied antiparallel to the magnetization direction of F. Hence, a Zeeman splitting $\sim g\mu_B B$ is induced in the N part of the junction. In the case of full spin-polarisation in F, only majority-type electrons, corresponding to the upper Zeeman level, can be injected from N into F. Hence, spin-flip excitation via resonant absorption of a microwave photon with energy $\hbar\omega = g\mu_B B$ is expected to increase the current over the N/F interface as long as the bias voltage is lower than the energy splitting, which will increase the apparent conductance of the junction [6]. Moreover, if the current direction is reversed, i.e. electrons are injected from F into N, a depression of the conductance at high current bias signals the overpopulation of the upper Zeeman level, which upon relaxation may lead to the spin-flip photoemission observed in previous experiments. According to the theoretical prediction the relative conductance change upon microwave absorption in such a point contact amounts to approximately 0.01%–1%, depending on the exact contact configuration. It is clear, that the effect strongly depends on the spin-polarisation in F, which should ideally be fully spin-polarised, e.g. in the case of Heusler alloys. For example Naidyuk and co-workers [12] observed a relative signal change of approximately 10% with fully spin-polarised $SmCo_5$ films. Fabricating atomic point contacts with these materials is, however, difficult because of their complex chemical nature and microstructure as well as high reactivity. Here, we investigate point contacts with ferromagnetic Co electrodes. Diverging values for the spin-polarisation of Co have been reported in the range between 10% and nearly 50% in the bulk, while in atomic contacts a higher spin-polarisation of 50%–70% has been measured recently [31]. The normal metal part of the junction is made of Pd, a strongly paramagnetic metal close to the Stoner criterion for ferromagnetism. Hence it is easily polarised in an external magnetic field. Moreover, unusually high g-factors have been reported for Pd [32–34], which would be beneficial to create a large energy splitting by applying small or moderate magnetic fields, i.e. lower than the coercive field of the F electrode.

4. Results and discussion

Before focusing onto Co/Pd hetero point contacts, we analyse the magnetoconductance of a pristine Pd MCBJ without magnetic electrodes. Figure 3(a) shows typical opening traces obtained upon reducing the contact diameter to the single-atom regime and breaking the junction until a tunnelling gap is observed. These individual opening traces can be compiled into conductance histograms showing the preferred conductance of atomic-scale point contacts made from Pd; the value of the preferred conductance is determined by the electronic valence of the material [35, 36]. The histogram reveals a relatively broad conductance peak of Pd single atom contacts around 1.8 G_0, where $G_0 = 2e^2/h$ denotes the conductance quantum. The results are consistent with previous measurements of Pd single atom contacts and in particular show that clean contacts are produced, because contamination, e.g. with hydrogen, would result in a strongly modified conductance histogram [37].

Magnetoconductance spectra are recorded in a single atom Pd contact at a conductance of $G \approx 0.71\ G_0$ at $T < 150$ mK. Figure 4(a) shows the differential conductance ($\mathrm{d}I/\mathrm{d}V$) of such a contact as a function of both applied magnetic field (B) and bias voltage (V). In quantum point contacts an unexpected plateau at the conductance at $\sim$0.7 G_0 has been reported [38–43], whose origin is still a matter of debate [44–50]. While there is

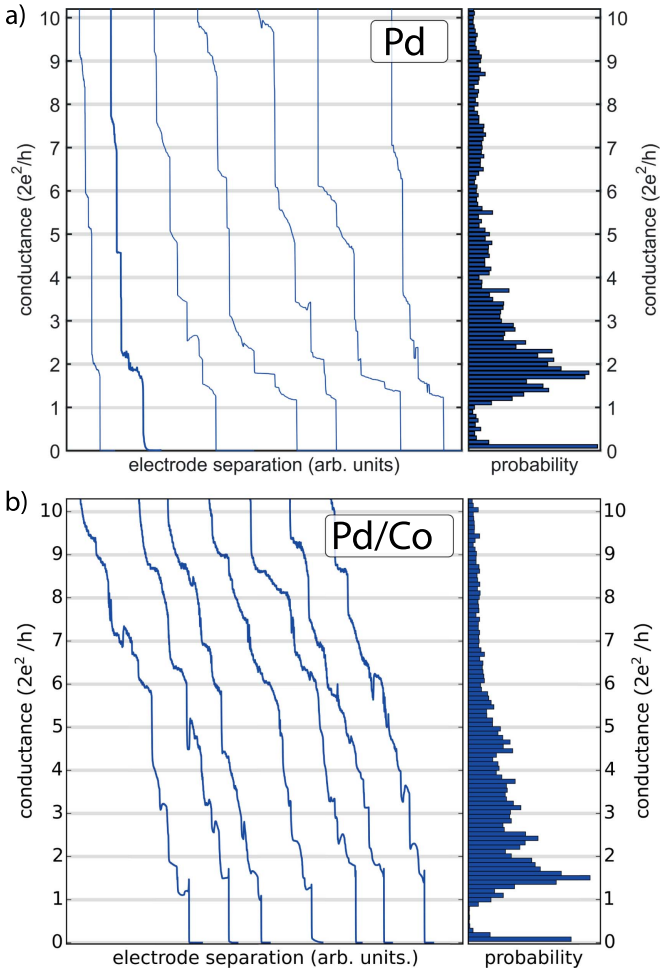

Figure 3. Selection of typical conductance traces while breaking MCBJs of (a) pristine Pd and (b) Pd/Co hetero contacts. A large number of these individual opening traces can be compiled into a conductance histogram shown in the right-hand panels for both Pd and Pd/Co junctions respectively. The histogram signals the preferred conductance values for each type of contact, i.e. the conductance of the single atom contact.

only a weak magnetic field dependence of the overall conductance, we note two distinct features in the point contact spectra of Pd at this conductance. The first one is a zero-bias anomaly (ZBA), which is present, when $B \neq 0$ and remains approximately constant when $|B|$ is increased. Different explanations have been proposed for the zero-bias conductance peak close to the 0.7 G_0 anomaly including the formation of a spontaneous spin-polarisation [49, 51], quasi-bound states leading to a Kondo impurity [48, 50, 52] and ferromagnetic spin-coupling [53]. We attribute the ZBA to a local magnetic impurity that develops in atomic contacts of some transition metal elements, even in clean contacts, as a result of the reduced dimensionality [54, 55]. This may lead to a Kondo-like feature with extremely high Kondo temperatures (up to 170 K) in the PC spectra. The occurrence of a Kondo feature is a common observation in Pd atomic contacts; a comparison of spectra and related Kondo temperatures is shown SI-3. It is not clear, however, why the ZBA is only present at finite magnetic field and absent at zero-field. It could be argued, that an out of plane polarisation of the Pd leads in vicinity of the atomic contact produces the ZBA instead of a local magnetic moment at the last atom and therefore a small, perpendicular magnetic field is required to rotate the magnetisation of the Pd leads.

The second, more important feature in the spectra in figure 4(a) are satellite peaks in the differential conductance at a bias voltage that increases linearly with the applied field. It is worth noting that this feature appears on top of the ZBA and is not a splitting of the Kondo resonance. Only very few contacts showed such behaviour and it is most prominent in the sample shown in figure 4(a). We attribute these peaks to a Zeeman splitting in the density of states of the Pd leads near the point contact. The fact that it can be observed in transport spectroscopy points to spin-dependent scattering at the Kondo impurity and may explain why it is observed only in contacts close to the 0.7 G_0 anomaly. The position of the Zeeman peaks extracted from the point contact spectra at different magnetic fields is shown in figure 4(b). Fitting the magnetic field dependence of this Zeeman peak (dashed line in figure 4(b)) yields an effective g-factor of $g = 1.93$, close to the value expected for a free

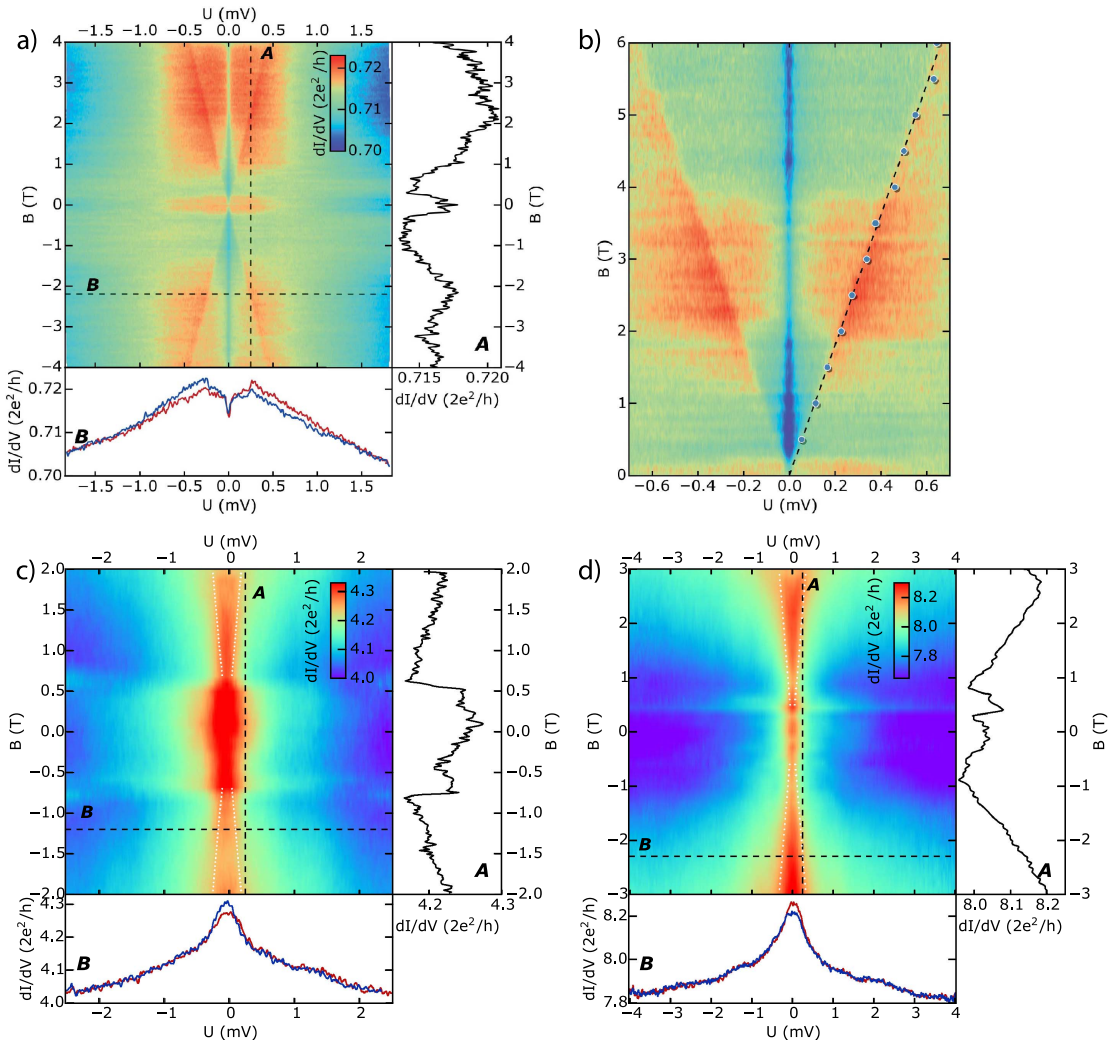

Figure 4. Differential conductance map of (a) 0.7 G_0 Pd point contact as a function of bias voltage and magnetic flux. In (b) symbols (●) mark the position of field dependent conductance steps is extracted from the spectra and the dashed line represents a linear Zeeman fit with g-factor $g = 1.93$. The panels (c) and (d) show differential conductance maps of hetero point contacts of different Pd/Co samples with zero-field conductance of (c) 4.3 G_0 and (d) 8.2 G_0 respectively. Both samples show a field dependent ZBA. As a guide to the eye the Zeeman splitting expected in Pd with a g-factor of 1.93 is superimposed on the broadening ZBA as a dotted line. The panels on the right and below show line traces along the field and bias axes at the positions (A and B) indicated by the dashed line in the pseudocolor plots. These cuts resemble the magneto-conductance and point contact spectra of the junctions compiled into a false colour image in the main panel.

electron gas. The g-factor is important in our experiment on Pd/Co point contacts to adjust the external field and hence the energy splitting to the resonance frequency of the microwave circuit.

We now turn to the study of hetero point contacts with a single interface between Pd and Co depicted in figure 2. The conductance histogram of these hetero-contacts in the atomic contact regime is shown in figure 3(b). In contrast to pristine Pd or Co MCBJs, we observe a more complex histogram with contributions from different contact conformations, i.e. the single atom contact may be formed between two Pd–Pd or Co–Co atoms as well as between one Pd and a Co atom, with different preferential conductance for each of the possibilities [56]. In comparison to the pristine Pd junctions in figure 3(a), the opening curves now show less pronounced plateaus in the few-atom regime and the shape of the plateaus changes from predominantly sloping to a distinct conductance increase at the end of most plateaus. This behaviour is related to the orbital structure of the material and is not normally observed in pure Pd or Co, which may indicate that the junction breaks at the Pd–Co interface and at least some atomic contacts are formed between Co and Pd atoms. Especially the last conductance plateau before the contact breaks into tunnelling shows both up- and downward slopes depending on the contact. The preferred conductance in the single atom regime is equally well defined as for pristine Pd junctions with a slightly reduced conductance value of 1.6 G_0, which is between the conductance known from both Co (1.3 G_0) and Pd (1.8 G_0) atomic contacts. This again may indicate that preferentially Pd–Co contacts are formed, which would be highly desirable but is not always realized since in many cases the contact breaks within the Pd or Co side of the interface. Because the mechanism of microwave absorption in energy-split spin-

subbands, outlined above, does not rely on having a single-atom contact, in the following we adjust the contact size to a diameter of a few atoms with a conductance below 10 G_0. In the few-atom regime, robust point contact spectra are obtained that do not vary much from contact to contact but their exact atomic configuration is normally not known. In particular the easy axis and magnetization state of the ferromagnetic Co electrode in the constricted region depends on the exact contact configuration, which is not directly accessible in our experiments. Therefore, physical interpretation of PC and magnetoconductance spectra rely on assumptions on the structural and magnetic contact configuration, which are based on a statistical analysis of many individual junctions, i.e. conductance histograms.

Figures 4(c) and (d) show two examples of PCS recorded at 50 mK in different Pd/Co hetero MCBJs with a zero-filed conductance of 8.2 G_0 and 4.3 G_0 respectively. The pseudocolor plots show the differential conductance of the PCs as a function of magnetic field and bias voltage. In both cases, we observe a ZBA in the conductance spectra that broadens with magnetic field. In contrast to pristine Pd PCs shown above, the spectra of Pd/Co hetero contacts are superimposed with a magnetoconductance background, which mainly originates from the parabolic anisotropic magnetoconductance and magnetic switching of Co domains in the leads above the coercive field of the electrodes. In Pd/Co hetero PCs, the magnetic-field independent, weak ZBA is not present or cannot be resolved on top of the larger, field-dependent feature. The broadening in the PCS with magnetic field is again linear and may be attributed to a Zeeman splitting in the DOS at the Pd/Co interface. However, the features are not as sharp as in the case of pure Pd contacts close to the 0.7 G_0 anomaly and in particular no clear Zeeman peaks can be distinguished. However, these peaks are not always observed, even in pure Pd junctions close to 0.7 G_0, where a peculiar spin-configuration may be present. In few-atom Co/Pd hetero PCs, where the contribution of several atoms in the cross-section of the contact contribute to the spectra, the larger number and arbitrary transmittance of the conduction channels broadens ZBA and Zeeman peaks. As a guide to the eye, the expected Zeeman splitting with the g-factor extracted from the measurement in figure 4(a) is marked as dashed line in figures 4(c) and (d). Although sharp satellite Zeeman peaks are not visible in Co/Pd hetero point contacts, the width of the zero-bias peak resembles the expected Zeeman splitting. If this is the case, resonant microwave absorption in the Zeeman split spin-subbands can be detected through characteristic changes in the transport characteristics at the ZBA of these contacts.

The lower panels in figure 4 show typical point contact spectra recorded at fixed magnetic fields indicated by a dashed line (B) in the respective false-colour representation above. Regardless of the contact size, the spectra recorded on different samples in figures 4(b) and (c) are very similar; in both cases a zero-bias conductance peak with similar magnitude and width is observed. This again indicates, that robust few-atom PCs can be fabricated with different contact diameters without changing the dominant physical mechanism. The panels on right in figure 4 show a cut through the data along the field axis at constant bias voltage, indicated by the labels (A) in each false-colour representation. In contrast to pristine Pd PCs, hetero contacts of Pd/Co show a much larger magnetoconductance, in particular at fields below 1 T; the coercive field of the Co electrodes in most contacts is around 550 mT. However, measurements on pure Co single-atom contacts and Co/Au heterojunctions showed strong magnetoconductance changes at fields up to 2 T [56]. In pristine Pd single atom contacts a spontaneous magnetization may emerge similarly to recent reports on Pt [55], which gives rise to the observed magnetoconductance behaviour. The magnetoconductance in Pd/Co heterojunctions can be attributed to a GMR-like effect, due to spin-dependent scattering of electrons at both Co–Pd interfaces. The conductance change due to spin-population inversion in Zeeman split spin-subbands is predicted to be in the order of 0.01%–1% depending on the details of the point contact [6]. Therefore, in order to reduce the parasitic magnetoconductance of the hetero PCs, the samples were designed such that both magnetic interfaces are separated well above the spin-diffusion length in Pd of about 25 nm at 4 K [30]. Hence placing the magnetic Co electrodes at a distance of 200 nm reduces the residual magnetoconductance due to spin-dependent interface scattering to less than 2%, which is lower than the parabolic AMR component of the magnetoconductance in perpendicular field up to 4 T. The remaining parabolic magnetoconductance background of the long Co leads has been subtracted in the following discussion of the data presented in figures 5(a)–(c).

After stabilizing a point contact and performing PCS at different magnetic fields, a microwave stimulus is applied to the junction at a fixed frequency and the spectroscopy measurements are repeated. According to the theory of spin-flip lasing in magnetic hetero PCs, the junction should display a distinct microwave-induced conductance change, when the resonance condition $\hbar\omega = g\mu_B B$ is matched. Despite the high stability of our setup and the possibility to analyse one particular, well-defined point contact over periods of several hours, most of the contacts change their geometry and hence their conductance upon application of large magnetic field or high voltage bias. Therefore only few PCs are stable enough to record a complete set of spectra in magnetic field with and without microwave stimulus. However, out of more than 90 stable F/N point contacts investigated in more than 15 samples with different materials for the F (Co, Ni, PdNi) and N (Ag, Cu, Pd, Au, Pt etc) components, only a fraction of five contacts showed a response to microwave stimulation, while most junctions remained totally unaffected until at high microwave powers, heating of the junction sets in. From our extensive

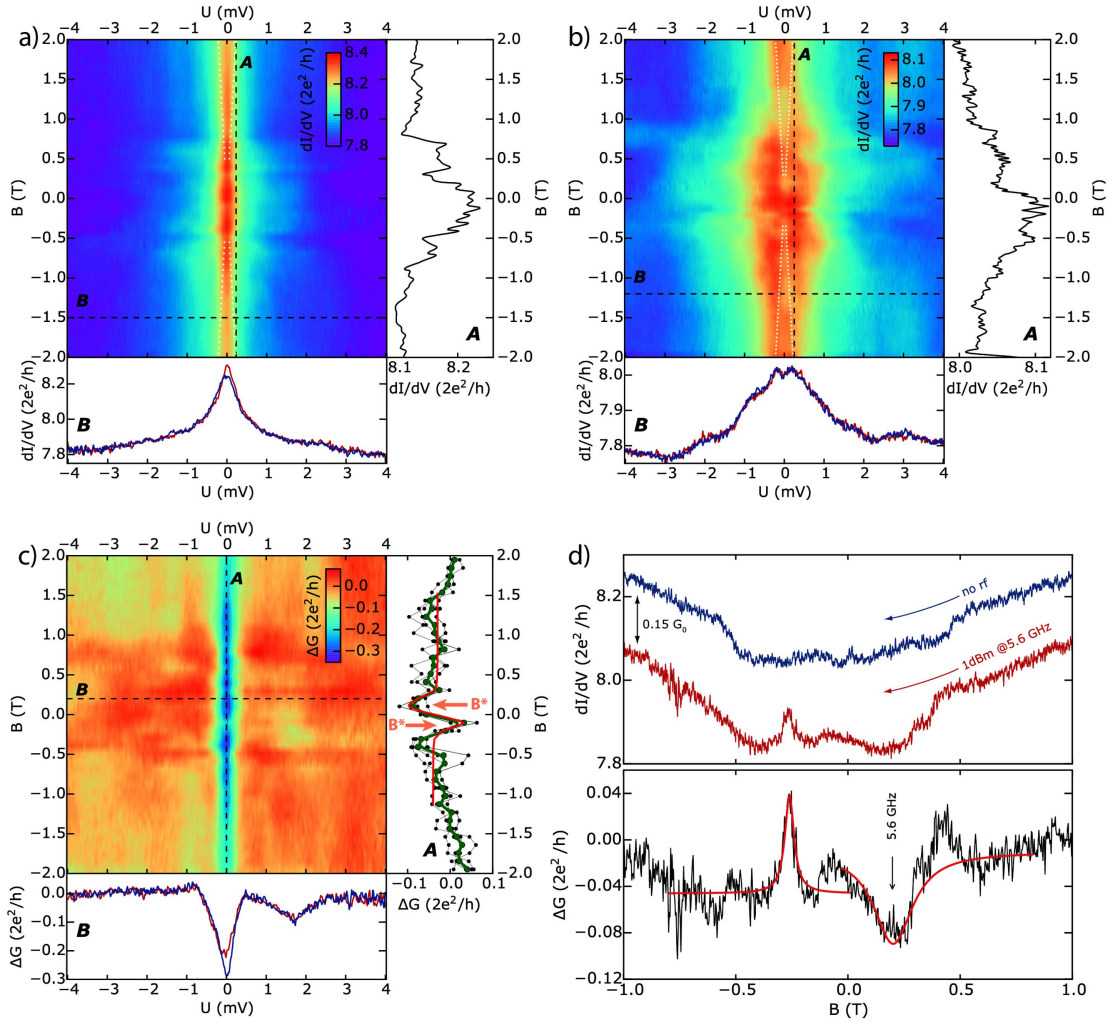

Figure 5. Differential conductance maps of a Pd/Co point contact at about 8.2 G_0 (a) without and (b) with microwave irradiation at a constant frequency of $f = 5.56$ GHz; the panels on the right and below again show the point contact spectra and magnetoconductance along the dashed lines (A, B) in the images. The zero-bias conductance peak in (a) broadens with the application external magnetic fields and is split in (b) under the application of a constant microwave stimulus (5.56 GHz @ −40 dBm). As a guide to the eye, the expected Zeeman splitting in Pd is superimposed on the images as dotted line. Panel (c) shows the conductance change due to microwave excitation of the contact, i.e. the difference between (a) and (b). A pronounced conductance dip/peak double feature appears at a field of ±200 mT at low bias voltage within the ZBA. The traces (-●-) in the right panel are sections through the data along the magnetic field axis at different bias voltages (*A*) from −25 to 25 μV in steps of 10 μV. The observed dip is present in all these traces and is unipolar in magnetic field. The green solid line is the median of the individual traces and the red line is a fit of equation (1) to the data. (d) consecutive magnetoconductance traces recorded with and without microwave stimulus, the curves are shifted for clarity. When the contact is irradiated with microwaves at constant frequency (5.6 GHz), again a dip/peak double feature is observed in the traces. The dip in the microwave induced signal conductance change is fitted using equation (1) to extract the resonance field and spin-relaxation rates.

studies we can conclude that spin-population inversion upon microwave absorption in magnetic point contacts is a *rare* phenomenon. Similar statistics have been reported for large point contacts between a sharp metallic (Cu) needle and a fully spin-polarised $SmCo_5$ film [12]. One possible reason is that, apart from the fact that the magnetisation in the F electrode should have a component antiparallel to the applied flux and the spin-polarisation should be high, it is not clear which conditions regarding the material- and interface properties on the microscopic level are required to observe this effect.

Measurements on junctions that showed a clear response to microwave irradiation are shown in figure 5. We restrict our discussion here to a Pd/Co point contact with zero-field conductance of 8.2 G_0 already shown in figure 4(d). For comparison, the differential conductance of this contact under fixed microwave stimulus at $f = 5.56$ GHz applied at a power of −40 dBm is shown in figure 5(b) together with the measurement without rf stimulation (figure 5(a)) on the same bias and magnetic field scales. The parabolic magnetoconductance background at bias voltages $|V| > 3$ mV, where the conductance spectra are almost featureless, has been subtracted. Under microwave irradiation pronounced conductance changes appear in the low bias region. In particular the ZBA broadens, and splits along the bias axis under the application of the microwave field. As a

guide to the eye, the expected Zeeman splitting is indicated again as dashed lines in figures 5(a) and (b). It matches the position of the conductance maxima observed in the point contact spectra under rf irradiation (see section B in figure 5(b)). Microwave absorption in Zeeman-split spin-subbands in the Pd region of the contact modifies the electron distribution and may even invert the population, which results in a spin-dependent conductance change across the interface with ferromagnetic Co layer. According to the theory outline above, the sign of the conductance change upon spin-inversion depends on the magnetisation of the F layer as well as the current- and external field direction, while its magnitude depends on material properties, such as the spin-polarisation in F as well as details of the contact, e.g. the effective PC volume and its normal resistance. In parallel magnetisation configuration a low bias conductance dip is expected as long as the voltage at the contact is lower than the field dependent Zeeman splitting of the spin-subbands in the Pd region of the contact. Hence in figure 5(b) a double peak structure is observed in the $\mathrm{d}I/\mathrm{d}V$ spectra and the position of the peaks follows the Zeeman splitting. The double peak vanishes when the reversal field of the Co electrode is reached. The microwave-induced conductance change in the $\mathrm{d}I/\mathrm{d}V$ spectra is shown in figure 5(c) in units of the conductance quantum. Pronounced conductance changes are observed in the low bias region, below 100 μV, while at larger bias voltages the conductance remains unaffected by microwave irradiation across the entire magnetic field range. This indicates that the contact configuration remained stable during the entire measurement cycle of 48 h, while repeatedly sweeping the magnetic field from 2 T to −2 T and recording $\mathrm{d}I/\mathrm{d}V$ spectra of the contact with and without microwave irradiation. This remarkable stability is one of the great advantages of atomic scale ballistic contacts used in this study, while diffusive contacts prepared by conventional PC techniques tend to destabilise within few minutes.

In the low bias regime a distinct conductance change indicates microwave absorption in the contact, when the resonance condition is matched. At the constant frequency stimulus of $\omega/2\pi = 5.56$ GHz the resonance field is at $B^* = 205$ mT, which corresponds to a Zeeman splitting of 23 μeV for a Pd contact with spin $= 1/2$ and the measured g-factor of 1.93. At this position we observe a pronounced dip in the conductance and a peak appears in the opposite field direction. The conductance as function of B has been extracted from the spectra and is shown in cross-sections A in a voltage range from −25 to 25 μV in intervals of 10 μV. All of them show a clear dip in the differential conductance with a magnitude in the order of −0.1 G_0 (≈1.2%), however with low resolution and considerable fluctuations, because the sections are extracted from I–V sweeps recorded while stepping the magnetic field from 2 T to −2 T in intervals of 100 mT. Nevertheless, a fit according to equation (1) to the averaged curves yields a resonance field of $|B^*| \approx 200$ mT, equivalent to a frequency of 5.4 GHz, which approximately matches the applied frequency. The observed feature is antisymmetric in magnetic field in accordance with the theory and quickly vanishes at finite bias, when $V > \hbar\omega^*$. The dip/peak double feature can be interpreted as absorption of microwave photons in Zeeman-split spin-bands. After saturating the Co electrodes in a large, positive field of 2 T and ramping back to the opposite field direction (−2 T), at positive field values the magnetisation of the ferromagnet is parallel to the external field and a conductance dip is observed close to zero bias upon populating the upper Zeeman level, when the microwave stimulus matches the resonance condition. When the field direction is reversed below the coercive field of the F electrode, the external field is antiparallel to the magnetisation in F and a conductance peak arises at the same resonance field due to the higher population of electrons with opposite spin in the upper Zeeman level. This gives rise to the observed dip/peak double feature similar to the situation shown in trace C in figure 1.

Individual magneto-conductance measurements at constant bias under microwave irradiation have been performed on contacts with sufficient stability. Since the magnetic configuration in the contact region is normally not known, we saturate the Co electrodes in a large external field to prepare them in a parallel state with respect to the applied field. The field is then ramped to the opposite direction and the conductance is monitored. The magnetisation direction of the Co electrode remains unchanged before reaching the coercive field in the opposite field direction. Hence, in a simplified picture, the external field is parallel to the magnetisation direction of the electrode at positive field values, while at low fields in the reverse direction the system is in the antiparallel state. Microwave-induced conductance changes are extracted from the sweeps by preparing a stable point contact and consecutively recording magnetoconductance data with and without rf irradiation of the contact at constant frequency.

The magneto conductance at zero dc-bias of the 8.2 G_0 contact is shown in figure 5(d). Again, in the upper panel, we compare measurements with and without microwave irradiation to disentangle microwave induced conductance changes and magnetoconductance changes as a result of reorienting the magnetisation direction of the Co electrodes at coercive fields of approximately 520 mT in this particular contact. Microwave absorption in the contact at zero-bias produces the peak-dip double structure already seen in section A in figure 5(c), which seems to be a robust feature in this contact. The field is again swept from positive the negative values. Hence the conductance dip occurs for a parallel configuration of the external field with respect to the magnetisation direction of the Co electrode, while the peak is observed in the antiparallel configuration upon reversing the external field. In this simplified picture, which ignores all microscopic details of the contact near the interface,

the experimental results correspond well to the theory. The magnetic configuration in the contact region on the atomic scale is in fact unknown and will change from contact to contact. In our interpretation we assume that the magnetic configuration of the Co electrode in the contact region changes reversibly with the applied field and remains unaffected by microwave irradiation. In particular ferromagnetic resonance (FMR) effects are avoided by restricting the frequency range to <10 GHz below typical FMR frequency of Co [57–59]. Individually fitting equation (1) to the dip and peak in the microwave induced conductance change yields slightly different values for the resonance fields. The peak occurs at a negative critical field of $B^*_1 = -230$ mT, while the dip is found on the opposite field axis at $B^*_2 = 198$ mT. These fields correspond to resonance frequencies of $\omega^*_1/2\pi = 6.3$ GHz and $\omega^*_2/2\pi = 5.4$ GHz respectively. This asymmetry can be caused by the fringing field of the Co electrode in the contact, which is superimposed on the external field and shifts the local field determining the Zeeman splitting in the Pd region of the contact. A second maximum appears in the signal at 480 mT, which can not be attributed to microwave absorption in the contact but originates from a different magnetic switching in both magnetic field sweeps. Notably the amplitudes of the microwave induced conductance features at B^*_1 and B^*_2 are similar, while their widths differs significantly. The amplitude of ~0.082 G_0 (1.05%) depends on natural constants and details of the contact, including the amplitude of the absorbed microwave field H_{rf}, the contact core volume Ω, the electron density n_0 in the N metal as well as its Fermi velocity ν_F and spin-flip rate ν_{sf}. The transport coefficient β in equation (1) has been empirically determined in previous reports to be 0.3 [6]. In contrast, the width of the resonance is given only by the Fermi velocity ν_F and the spin flip rate ν_{sf} in Pd is obtained from the fit in figure 5(d). A fit to the conductance dip yields a spin-flip rate $\nu_{sf} = 1.8 \times 10^{10}$ s^{-1}, while for the narrow conductance peak we obtain $\nu_{sf} = 5.2 \times 10^9$ s^{-1}. These values for ν_{sf} are in the range reported in the literature for Pd [60]. The observed conductance change upon microwave irradiation of the contact in the low bias regime is well described by the theory of microwave absorption in magnetic hetero point contacts and supports the hypothesis that this feature is associated to a spin-flip transition in Zeeman-split spin sub-bands, stimulated by the microwave field. The relative conductance change up to 1% observed in ballistic contacts is large compared to previous reports, which shows that atomic-scale ballistic PCs not only provide superior stability but are also more sensitive to detect the population inversion in the spin-subbands upon microwave absorption. The drawback of ballistic, atomic contacts is that spin-flip photoemission is very weak, due to the low volume of the contact core, where the critical current density is reached. Hence direct detection of photoemission from these contacts using conventional cryogenic microwave detectors remains a challenging task. Therefore emission of microwave photons in strongly dc-biased junctions can be revealed only indirectly via the associated conductance change. The emissive high bias region, where the voltage at the contact exceeds the threshold voltage V^* for photoemission, depends on microscopic details of the junction and the contact materials. Spin-population inversion due to injection of hot, spin-polarised electrons in the energy split spin-subbands is expected for current densities exceeding several 10^7 A cm^{-2}, which has been demonstrated to be feasible in short, diffusive F/N heterocontacts. In ballistic Co/Pd contacts with a cross-section of four to five Pd atoms, such current densities are already reached at excitation voltages below 500 μV, while these contacts tolerate voltage up to few tens of mV corresponding to several times 10^9 A cm^{-2} before instabilities lead to geometric reordering in the junction due to large electromigrative forces. Usually contact reorganisation at high current bias and large magnetic fields is irreversible and associated to conductance changes in the order of the conductance quantum. In this case, the analysis of subtle conductance changes ($\Delta G \sim 0.1\ G_0$) upon microwave irradiation of the contact becomes increasingly difficult. We investigate the signature of spin-flip photoemission in the PC conductance in contacts with sufficient stability, i.e. where no contact reorganisation takes place during the measurement, which often results in a sudden, permanent conductance change, i.e. when the magnetic field is swept. Figure 6 shows the conductance of a 4.3 G_0 contact recorded in two subsequent magnetic field sweeps as well as the microwave-induced conductance change at constant frequency of $\omega_{rf}/2\pi = 10$ GHz. The measurement was performed at a constant current bias of -6 μA, which corresponds to a current density of approximately $j = 5 \times 10^9$ A cm^{-2} in a three-atom contact. The negative current direction denotes a current driven from the Pd side of the junction into the Co electrode. In this configuration a spin-population inversion is achieved at parallel alignment of the external field and the Co electrode's magnetisation by depopulating the lower Zeeman level, when a current is directed from N into F [12]. Emission of a microwave photon upon spin-population inversion is signalled by an increase in the contact resistance. It has been demonstrated recently that this process may be stimulated in nature and is only visible under microwave irradiation, when the resonance condition is matched. The microwave-induced conductance change in figure 6, shows a clear dip in the conductance at $B^* = 385$ mT, which is unipolar in magnetic field in accordance with the theory. Markedly, a small dip is also observed in the magnetoconductance at nearly the same resonance field, when the contact is not irradiated with microwaves because the population inversion is created via current injection of electrons at high current bias, and relaxation may occur via spontaneous spin-flip emission or magnonic transitions. The observation of this feature indicates a resonant amplification of the electromagnetic ac field in the junction at the resonance field, when the boundary conditions for spin-flip photoemission are matched.

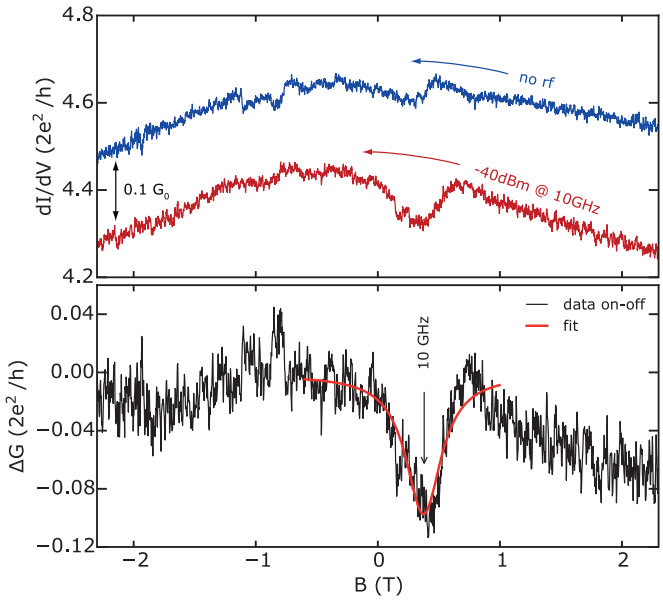

Figure 6. Consecutive magnetoconductance traces recorded with and without microwave stimulus of −40 dBm at a frequency of 10 GHz. The curves are vertically displaced for clarity by 0.1 G_0. When the contact is irradiated with microwaves at constant frequency (10 GHz), a dip is observed in the traces. The dip in the microwave induced signal conductance change is fitted with equation (1) to extract the resonance field of $B^* = 385$ mT and the spin-flip rate $\nu_{sf} = 3 \times 10^{10}$ s^{-1} of the contact.

The microwave induced conductance change in figure 6 shows a clear dip at the resonance field $B^* = 385$ mT; fitting equation (1) to the data at resonance frequency of $\nu^* = 10.42$ GHz yields a spin-flip rate of $\nu_{sf} = 3.1 \times 10^{10}$ s^{-1}. There is again a small deviation of the excitation frequency at 10 GHz and the resonance field observed in the measurement, which is likely to be caused by the fringing field of the cobalt electrode or its direct coupling to the Pd layer, which results in an increased Zeeman splitting. In contrast, non-radiative relaxation of hot electrons above excited Zeeman state would lead to a reduction of the resonance frequency. The spin-flip rates extracted from the data correspond to spin relaxation times of 30–100 ps, which is in the range of values reported in the literature [61] for polyvalent metals and determined for Pd via CESR measurements [62, 63] as well as spin-injection experiments [64]. Together with the fact that pronounced conductance changes are observed only under microwave irradiation close to the resonance frequency, this again supports the hypothesis that direct spin-flip transitions in Zeeman-split spin sub-bands can be triggered. The emission of microwave photons upon relaxation of the non-equilibrium spin-population as predicted by the theory still remains to be shown. However, both the absorption of microwave photons as well as the current-pumped spin-asymmetries in ballistic Pd/Co heterocontacts produced large conductance changes compared to previous studies on diffusive contacts, even those based on strongly spin-polarised alloys.

In our study only a fraction of all contacts showed a signature of spin-accumulation and responded to microwave irradiation. A clear disadvantage of few-atom ballistic junctions in comparison to diffusive point contacts prepared by other means is that the magnetic configuration at the interface often remains unknown. Ensembles of point contacts should be studied further to increase the low observation rate and fabricate devices where spin-flip photoemission can be directly measured. Moreover, future work in individual, ballistic PCs will focus on minimising the effect of competing relaxation mechanisms, such as magnon scattering, as well as on evaluating the role of interface properties, spin-polarisation and magnetic ordering in the contact region.

5. Conclusions

In summary we demonstrated that ballistic, few atom hetero point-contacts composed of a ferromagnetic and a normal, paramagnetic metal are well suited to investigate non-equilibrium spin-distribution and relevant relaxation phenomena. In particular the absorption and emission of microwave photons in Zeeman-split spin sub-bands was demonstrated experimentally by analysing the associated conductance change of a number of different contacts on the basis of semi-classical theory recently developed and applied to diffusive point contacts. We demonstrated that the microwave-induced conductance change in ballistic Pd/Co hetero-junctions is much larger than previously observed in the diffusive regime. Moreover, the mechanically controlled break-junction technique serves to produce highly stable point contacts, which allowed an in-depth study of the new

phenomena of absorption and emission of microwave photons in energy split spin-subbands. The microwave-induced conductance changes observed in Co/Pd contacts are well described within the simple theoretical framework developed recently. Due to its high sensitivity to a change in the spin distribution, ballistic hetero-contacts are the preferred tool to further investigate these questions. However, so far only a fraction of all contacts showed the signature of inverse spin-accumulation and responded to microwave irradiation, possibly because the microscopic details as well as material and interface requirements to observe this effect are not fully clear. Future work in individual, ballistic PCs will focus on minimising the effect of competing relaxation mechanisms and evaluating the role of interface properties, spin-polarisation and magnetic ordering in the contact region. Ultimately, these studies will reveal the design rules to construct miniaturised, highly tunable microwave emitters with giant intensity based on point-contact arrays, which may be highly beneficial in communication, memory storage and sensing devices. In this respect, also ensembles of point contacts should be studied to increase the low observation rate and fabricate devices where spin-flip photoemission can be directly measured optically.

Acknowledgments

We thank Anatoli Kadigrobov (Institute of Theoretical Physics III, Ruhr-University, Bochum) and Vladislav Korenivski (Royal Institute of Technology, Stockholm) for fruitful discussions and their support regarding the theoretical concept of spin-flip lasing in metallic junctions. We gratefully acknowledge financial support via the EU-FP7 ICT-FET open programme (STELE 225955), from the German Research Foundation (DFG) via the research grant (PI 1103/1) and the Zukunftskolleg of the University of Konstanz.

Author contributions

SE, MK, FS, HF-P and TP performed the experiments. TP and ES planned the project and advised the students. All authors discussed the results and prepared the manuscript together.

References

[1] Chumak A V, Vasyuchka V I, Serga A A and Hillebrands B 2015 *Nat. Phys.* **11** 453
[2] Hoffmann A and Schultheiss H 2015 *Curr. Opin. Solid State Mater. Sci.* **19** 253
[3] Stamps R L *et al* 2014 *J. Phys. D: Appl. Phys.* **47** 333001
[4] Zutic I, Fabian J and Das Sarma S 2004 *Rev. Mod. Phys.* **76** 323–410
[5] Bader S D and Parkin S S P 2010 *Annu. Rev. Condens. Matter Phys.* **1** 71
[6] Kadigrobov A M, Shekhter R I, Aronov I, Kulinich S I, Pulkin A and Jonson M 2011 *Low Temp. Phys.* **37** 925
[7] Kadigrobov A, Ivanov Z, Claeson T, Shekhter R I and Jonson M 2004 *Europhys. Lett.* **67** 948
[8] Kadigrobov A, Shekhter R I and Jonson M 2005 *Low Temp. Phys.* **31** 352
[9] Kadigrobov A M, Shekhter R I, Kulinich S I, Jonson M, Balkashin O P, Fisun V V, Naidyuk Y G, Yanson I K, Andersson S and Korenivski V 2011 *New J. Phys.* **13** 023007
[10] Shekhter R I, Kadigrobov A M, Jonson M, Smotrova E I, Nosich A I and Korenivski V 2011 *Opt. Lett.* **36** 2381
[11] Gulyaev Y V, Zil'berman P E, Krikunov A I, Panas A I and Epshtein E M 2007 *JETP Lett.* **85** 160
[12] Naidyuk Y G *et al* 2012 *New J. Phys.* **14** 093021
[13] Kadigrobov A M, Shekhter R I, Kulinich S I and Jonson M 2011 *Physics and Simulation of Optoelectronic Devices XIX Proc. SPIE Int. Soc. Opt. Eng.* 79331G
[14] Korenivski V, Iovan A, Kadigrobov A and Shekhter R I 2013 *Europhys. Lett.* **104**
[15] Gulyaev Y V, Zil'berman P E, Malikov I V, Mikhailov G M, Chigarev S G and Epshtein E M 2012 *J. Commun. Technol. Electron.* **57** 329
[16] Gulyaev Y V, Zilberman P E, Malikov I V, Mikhailov G M, Panas A I, Chigarev S G and Epshtein E M 2011 *JETP Lett.* **93** 259
[17] Gulyaev Y V, Vilkov E A, Zil'berman P E, Mikhailov G M, Chernykh A V and Chigarev S G 2014 *JETP Lett.* **99** 508
[18] Gulyaev Y V, Vilkov E A, Zil'berman P E, Mikhailov G M, Chigarev S G and Epshtein E M 2013 *JETP Lett.* **98** 96
[19] Gulyaev Y V, Zilberman P E, Mikhailov G M and Chigarev S G 2014 *JETP Lett.* **98** 742
[20] Vilkov E A, Gulyaev Y V, Zil'berman P E, Malikov I V, Mikhailov G M, Panas A I, Chernykh A V and Chigarev S G 2015 *J. Commun. Technol. Electron.* **60** 1044
[21] Gulyaev Y V, Zil'berman P E and Chigarev S G 2015 *J. Commun. Technol. Electron.* **60** 411
[22] Gulyaev Y V, Vilkov E A, Zil'berman P E, Mikhailov G M, Chernykh A V and Chigarev S G 2015 *J. Commun. Technol. Electron.* **60** 1016
[23] Naidyuk Y G and Yanson I K 2005 *Point-Contact Spectroscopy* 1st edn (New York: Springer)
[24] Kadigrobov A M, Shekhter R I, Aronov I, Kulinich S I, Pulkin A and Jonson M 2012 *Low Temp. Phys.* **38** 183
[25] Kadigrobov A M, Shekhter R I and Jonson M 2012 *Low Temp. Phys.* **38** 1133
[26] Gulyaev Y V, Zil'berman P E, Krikunov A I, Panas A I, Chigarev S G and Epshtein E M 2008 *J. Commun. Technol. Electron.* **53** 1345
[27] Tao X D, Feng Z, Miao B F, Sun L, You B, Wu D, Du J, Zhang W and Ding H F 2014 *J. Appl. Phys.* **115** 17C504
[28] Tang Z Y, Kitamura Y, Shikoh E, Ando Y, Shinjo T and Shiraishi M 2013 *Appl. Phys. Express* **6** 083001
[29] Foros J, Woltersdorf G, Heinrich B and Brataas A 2005 *J. Appl. Phys.* **97** 10A714
[30] Kurt H, Loloee R, Eid K, Pratt W P and Bass J 2002 *Appl. Phys. Lett.* **81** 4787
[31] Sivkov I N, Brovko O O, Bazhanov D I and Stepanyuk V S 2014 *Phys. Rev.* B **89** 075436
[32] Mueller F M, Freeman A J and Koelling D D 1970 *J. Appl. Phys.* **41** 1229
[33] Hornfeld S, Ketterso J B and Windmill L R 1969 *Phys. Rev. Lett.* **23** 1292
[34] Fischer G, Herr A and Meyer A J P 1968 *J. Appl. Phys.* **39** 545
[35] Scheer E, Agrait N, Cuevas J C, Yeyati A L, Ludoph B, Martin-Rodero A, Bollinger G R, van Ruitenbeek J M and Urbina C 1998 *Nature* **394** 154

[36] Agrait N, Yeyati A L and van Ruitenbeek J M 2003 *Phys. Rep.-Rev. Section Phys. Lett.* **377** 81–279
[37] Csonka S, Halbritter A, Mihaly G, Shklyarevskii O I, Speller S and van Kempen H 2004 *Phys. Rev. Lett.* **93** 016802
[38] Ren Y, Yu W W, Frolov S M, Folk J A and Wegscheider W 2010 *Phys. Rev.* B **82** 045313
[39] Sarkozy S, Sfigakis F, Das Gupta K, Farrer I, Ritchie D A, Jones G A C and Pepper M 2009 *Phys. Rev.* B **79** 161307
[40] Koop E J, Lerescu A I, Liu J, van Wees B J, Reuter D, Wieck A D and van der Wal C H 2007 *J. Supercond. Novel Magn.* **20** 433
[41] DiCarlo L, Zhang Y, McClure D T, Reilly D J, Marcus C M, Pfeiffer L N and West K W 2006 *Phys. Rev. Lett.* **97** 036810
[42] Cronenwett S M, Lynch H J, Goldhaber-Gordon D, Kouwenhoven L P, Marcus C M, Hirose K, Wingreen N S and Umansky V 2002 *Phys. Rev. Lett.* **88** 226805
[43] Appleyard N J, Nicholls J T, Pepper M, Tribe W R, Simmons M Y and Ritchie D A 2000 *Phys. Rev.* B **62** R16275
[44] Bauer F, Heyder J, Schubert E, Borowsky D, Taubert D, Bruognolo B, Schuh D, Wegscheider W, von Delft J and Ludwig S 2013 *Nature* **501** 73
[45] Burke A M, Klochan O, Farrer I, Ritchie D A, Hamilton A R and Micolich A P 2012 *Nano Lett.* **12** 4495
[46] Micolich A P 2011 *J. Phys.: Condens. Matter* **23** 443201
[47] Lunde A M, De Martino A, Schulz A, Egger R and Flensberg K 2009 *New J. Phys.* **11** 023031
[48] Rejec T and Meir Y 2006 *Nature* **442** 900
[49] Reilly D J 2005 *Phys. Rev.* B **72** 033309
[50] Meir Y, Hirose K and Wingreen N S 2002 *Phys. Rev. Lett.* **89** 196802
[51] Thomas K J, Nicholls J T, Simmons M Y, Pepper M, Mace D R and Ritchie D A 1996 *Phys. Rev. Lett.* **77** 135
[52] Heyder J, Bauer F, Schubert E, Borowsky D, Schuh D, Wegscheider W, von Delft J and Ludwig S 2015 *Phys. Rev.* B **92** 195401
[53] Aryanpour K and Han J E 2009 *Phys. Rev. Lett.* **102** 195401
[54] Gentile P, De Leo L, Fabrizio M and Tosatti E 2009 *Europhys. Lett.* **87** 27014
[55] Strigl F, Espy C, Buckle M, Scheer E and Pietsch T 2015 *Nat. Commun.* **6** 6172
[56] Egle S, Bacca C, Pernau H F, Huefner M, Hinzke D, Nowak U and Scheer E 2010 *Phys. Rev.* B **81** 134402
[57] Beaujour J M L, Chen W, Kent A D and Sun J Z 2006 *J. Appl. Phys.* **99**
[58] Kornev Y V, Vuntesme V S and Batrakov L M 1971 *Phys. Met. Metallogr.* **31** 92–8
[59] Schoeppner C, Wagner K, Stienen S, Meckenstock R, Farle M, Narkowicz R, Suter D and Lindner J 2014 *J. Appl. Phys.* **116** 033913
[60] Fabian J and Das Sarma S 1999 *J. Vac. Sci. Technol.* B **17** 1708
[61] Bass J and Pratt W P 2007 *J. Phys.: Condens. Matter* **19** 183201
[62] Fabian J and Das Sarma S 1998 *Phys. Rev. Lett.* **81** 5624
[63] Feher G and Kip A F 1955 *Phys. Rev.* **98** 337
[64] Poli N, Morten J P, Urech M, Brataas A, Haviland D B and Korenivski V 2008 *Phys. Rev. Lett.* **100** 136601